(Preprint) AAS 21-243

A RAPID TARGET-SEARCH TECHNIQUE FOR KBO EXPLORATION TRAJECTORIES

Miguel Benayas Penas[*], Kyle M. Hughes[†], Bruno V. Sarli[‡], Donald H. Ellison[§], and Kevin J. Cowan[¶]

A rapid, grid-based, target-search algorithm is presented to find candidate sequences of small-body encounters for mission design. The algorithm is especially relevant for cases with large combinatorial spaces. In this paper, the algorithm is used to identify candidate flyby sequences of multiple Kuiper-Belt Objects (KBOs). Before reaching the first KBO in the sequence, the trajectories in this paper first use gravity assists at one or more of the giant planets to pump-up their orbital energy—reducing launch C_3. The target-search algorithm consists of four sequential steps: (1) parameter definition, (2) fine-tuned Lambert-based grid search of ballistic trajectories visiting one KBO, (3) rapid, ΔV-based proximity search for additional KBOs using the state transition matrices (STMs), and (4) trajectory optimization of the most promising KBO sequences using the Evolutionary Mission Trajectory Generator (EMTG). The paper also defines an empirical-based process to characterize the maximum step size for the target arrival dates in the Lambert grid search. Lastly, a candidate mission to two KBOs is presented. The results indicate that the ΔV computed from the STM propagations is not representative of the final ΔV computed in EMTG; however, it does serve as a useful 'reachability' metric to identify nearby KBOs.

INTRODUCTION

Identifying the possible sequences of body encounters for a spacecraft (pathfinding) is often impractical to compute exhaustively. This is particularly true for missions seeking multiple flybys of some unknown set of bodies out of a large population— e.g. KBOs, main-belt asteroids, NEAs, and Jupiter Trojans. Such large combinatorial spaces will dramatically slow down the trajectory search process—potentially taking months of computation time. Using a pathfinding filter beforehand may sharply reduce the computation time needed.

This paper presents a rapid target-search algorithm (TSA) for trajectories to multiple KBOs, which make up a relatively unknown region formed by remnants of the original Solar System[1] . The TSA aims to spot a subset of flyable body encounter sequences with a small fraction of the time

[*]Aerospace Engineer, Physics Department, Catholic University of America, 620 Michigan Ave. NE, Washington, District of Columbia, 20064, USA.

[†]Aerospace Engineer, Navigation and Mission Design Branch, NASA Goddard Space Flight Center, Greenbelt, MD, 20771, USA.

[‡]Aerospace Engineer, HelioSpace, 932 Parker St. Suite 2, Berkeley, CA, 94710, USA.

[§]Aerospace Engineer, Navigation and Mission Design Branch, NASA Goddard Space Flight Center, Greenbelt, MD, 20771, USA.

[¶]Education Fellow + Lecturer, Faculty of Aerospace Engineering, Delft University of Technology, Postbus 5058, Delft, South Holland, 2600 GB, The Netherlands.

required to explore the whole combinatorial space. The TSA combines the grid search technique[2–4] with the recent STM-linearization method for KBO[5,6] for maneuver calculation.

The TSA could be applied to other trajectory design problems with a large combinatorial number for body encounters such as exploration missions to NEAs, Jupiter Trojans, or Jovian Moons.

TARGET-SEARCH ALGORITHM

The TSA consists of a four-step sequence. First, the mission constraints are specified. Second, a Lambert-based grid search of ballistic trajectories visiting one KBO is fine-tuned and run. Third, a rapid, ΔV-based proximity search for additional KBOs is conducted by linearizing the STMs from Kepler's problem. Finally, trajectory optimization of the most promising KBO sequences is applied using EMTG for pathsolving.

1. Mission constraints

The parameters used in this study for KBO exploration trajectories are summarized in Table 1. The high C_3 bound used is intended to accommodate an increased C_3 after a prior gravity-assist sequence, to pump up the orbital energy before a final Earth flyby. Such a precedent gravity-assist sequence is represented in these trajectory results as the initial departure body.

Table 1. Summary of key parameters used in the target search

Parameter	Value
Earliest launch date	01/01/2026
Latest launch date	12/31/2041
Maximum TOF to reach first KBO [years]	15
Maximum TOF of the whole mission [years]	20
Maximum ΔV [km/s]	2
Maximum launch C_3 [km^2/s^2]	500
Minimum launch C_3 [km^2/s^2]	49

In addition, two assumptions regarding the number of revolutions and planet flyby sequences were made for the Lambert-based grid search. These two assumptions are presented in Table 2.

Table 2. Number of revolutions and flyby sequences chosen for the KBO exploration trajectory search.

Parameter	Value
Number of revolutions allowed for Lambert problem	0
Planet flyby sequences	E-J, E-J-U, and E-J-N

The Table 2 values were set to minimize computation time while still considering a broad solution space. Not many multi-revolution trajectories were expected to happen for those chosen flyby sequences, considering they have to reach the Kuiper Belt within 15 years. Regarding the flyby sequences, E-J was included due to Jupiter's enormous gravitational pull. Neptune and Uranus were included to bend to the trajectory in the outer Solar System and thus provide a wider variety of approach geometries as the spacecraft enters the Kuiper Belt, Figure 1, increasing chances of encountering KBOs.

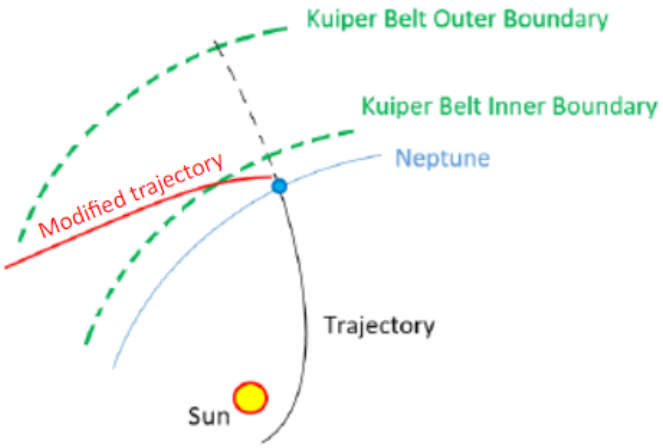

Figure 1. Schematic illustrating the advantages of including Neptune (or similarly, Uranus) for gravity assist in KBO search. Performing a flyby about Neptune bends the black trajectory turning it into the 'modified trajectory' in red, changing the trajectory's approach into the Kuiper Belt and improving the odds of finding trajectories that can encounter multiple KBOs.

2. Lambert-based grid search of ballistic trajectories

A Lambert grid search of ballistic trajectories to a single KBO is computed, using a patched-conic model for planetary gravity assists and a Kepler propagator for interplanetary cruise[7] . The gravity assists are computed using a C_3-matching algorithm[8] . Given an incoming flyby trajectory, the C_3-matching algorithm computes all the possible outgoing flyby ballistic trajectories to the target body through its discretized orbit. Then, the C_3-matching algorithm outputs the outgoing trajectories that match the incoming flyby trajectory's C_3 with a feasible bending angle.

To fine-tune the step size for the target-body arrival dates in the Lambert grid search, a systematic, empirically-based process is previously implemented to minimize both computations and missing solutions. This process supposes, along with the TSA, the key contribution of this paper. There is a plethora of literature using grid search for mission design[9–13] . Despite the abundance of work, publications usually do not discuss how the orbital time step values were assigned. The process hereunder explained tries to bridge the gap between algorithm design and actual implementation in this regard.

The empirical process consists of finding the minimum radius of curvature from all the C_3-TOF curves for each adjacent pair of bodies in a flyby sequence. The minimum radius of curvature is used as a representative minimum step size to characterize the curve; and thus, is used as the target arrival date step size in the Lambert grid search to avoid any missed solutions in the C_3-matching algorithm. The radius of curvature (R) is defined in Eq. (1)[14] .

$$R = \frac{|\ddot{C}_3|}{\left(1 + C_3^2\right)^{3/2}} \quad ; \quad C_3 = C_3(TOF) \tag{1}$$

In order to compute the minimum radii of curvature, outcoming C_3-TOF curves are defined using ultra-fine time steps for the planetary orbits. Then, trajectories of every C_3-TOF curve are sorted into the different solution families. Finally, radii of curvature are calculated from localized fifth-order polynomial curve fits in sets of 10 points across the entire curve.

It is noteworthy that one complication in this approach is that, for 180-degree transfers between bodies, a spike appears in the C3-TOF curve, which seems to be representative of a vertical asymptote. Such locations would have very low radius of curvature, which is not a useful minimum for the grid search step size. Thus, trajectories with transfer angles within 2 degrees of 180 degrees are ignored.

The parameter values used to define the ultra-fine arrival orbit discretizations for all the flyby-target body couples are summarized in Table 3. Launch and arrival C_3 were calculated with the aid of a Tisserand graph[15] .

Table 3. Parameter values used for the the ultra-fine arrival orbit discretizations.

	Earth-Jupiter	**Earth-Saturn**	**Earth-Uranus**	**Earth-Neptune**	**Earth-Pluto**	**Jupiter-Saturn**	**Jupiter-Neptune**
Minimum Relative Launch C_3 $[km^2/s^2]$	49	81	100	100	121	1	9
Minimum Relative Arrival C_3 $[km^2/s^2]$	25	25	9	9	25	1	1
Launch Window [yrs]	1.5	1.5	1.5	1.5	1.5	12	12
Maximum TOF [yrs]	10	15	20	20	20	20	20
Orbit Resolution [days]	1,0.43	1,1	1,1	1,1	1,1	12,1	12,1
Max ΔV [km/s]	0	0	0	0	0	0	0

Jupiter's step size was set to 0.43 days (corresponding to 10,000 grid points per orbit) for the E-J scenario in Table 3 since Jupiter is much closer to Earth than the rest of the bodies, and having the same 1-day value would lead to a coarser orbit discretization.

The J-S and J-N scenarios were included to compare with E-S and E-N, respectively, and check whether or not varying the departure may affect the minimum radius of curvature value for the target-body orbit. The 12-day discretization was chosen to have the same number of grid points as the E-J and E-S scenarios.

All of the C_3-TOF curves obtained from Table 3 are classified into different families using the parameters provided in Table 4 . The reason is to avoid false low radius of curvature in the vicinity of a 180-degree transfer angle when computing the radii of curvature. In that region, solutions belonging to the two different sides of the asymptote could be wrongly interpreted as a single curve if no sorting criterion is applied.

Table 4. Trajectory sorting criteria. The k parameter is an universal variable defined in[16] .

Sorting Criterion	**Key Parameter**
Launch Date	Launch Date
Type of Conic	Specific Energy
Number of Revolutions	TOF/Orbit Period
Prograde/Retrograde	Cross Product Sign of **r**,**v**
High/Low Energy	k Parameter
Type I or II	Transfer Angle Over/Below 180 degrees

The results of the ultra fine-tune phase lead to an empirical law for semi-major axis versus time step size, summarized in Table 5 and illustrated Figure 2.

Table 5. Results attained from the E-J, E-S, E-U, E-N and E-P scenarios in the parameter fine-tuning phase.

	Jupiter	Saturn	Uranus	Neptune	Pluto
Orbit Period [Years]	11.86	29.45	84.02	164.80	247.74
Orbit Period [Days]	4333	10756	30687	60190	90487
Semi-major Axis [AU]	5.20	9.54	19.19	30.07	39.49
Step Size [Days]	7.04	39.58	79.02	371.02	1297.09
Grid Points Per Orbit	615.46	271.75	388.35	162.23	69.76
Log Step Size	0.84	1.59	1.90	2.57	3.11

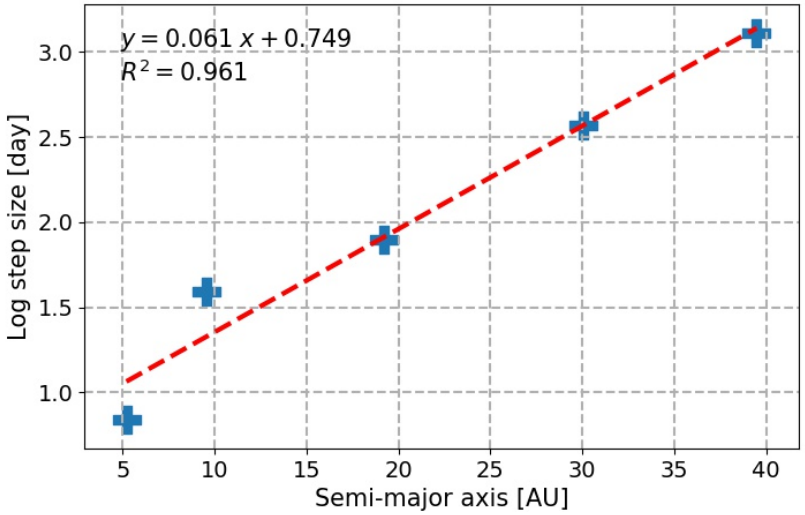

Figure 2. Fine-tuned time step with respect to semi-major axis.

Furthermore, the computed step sizes for Jupiter-Saturn and Jupiter-Neptune scenarios of Table 3 were 40.40 and 378.87 days respectively, quite close to the 39.58 and 371.02 days for E-S and E-N of Table 5. Thus, for this work, it was assumed the departure does not significantly affect the arrival body discretization.

The Lambert grid search of ballistic trajectories to one KBOs was run based on the empirical law of fine-tuned orbit step sizes provided in Figure 2. Earth step size was set to the conservative value of 1 day. The results are presented in Figure 3.

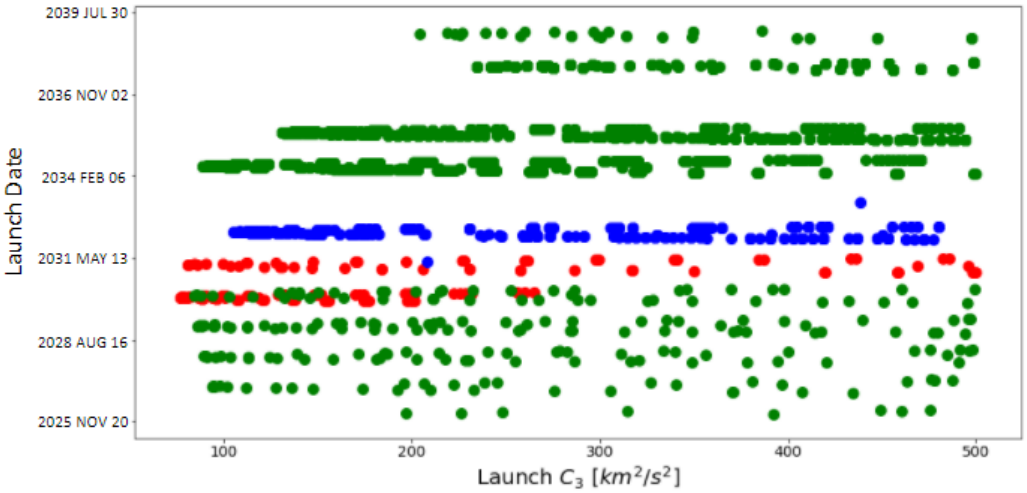

Figure 3. Launch C_3 versus launch date plot for the first grid search results. Red dots stand for E-J trajectories, while green and blue dots represent E-J-U and E-J-N scenarios respectively.

3. Rapid, ΔV-based proximity search using STMs

The addition of extra KBO encounters in the vicinities of the ballistic trajectories coming from the Lambert grid search is evaluated with a proximity search. Linear propagations of the STMs assuming a Keplerian, two-body propagator[5,6] were used to calculate maneuvers. The resulting total ΔVs are interpreted in the TSA as a reachability metric, as the linearized ΔV is not always an accurate representation of the true ΔV. The algorithm is depicted in Figure 4.

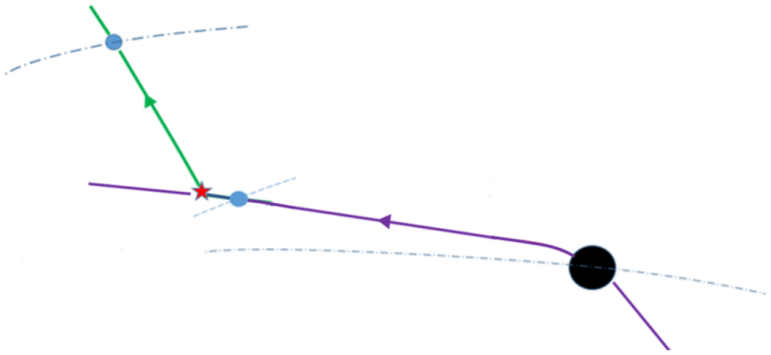

Figure 4. Conceptual image of the proximity search to add a second KBO. The baseline trajectory is depicted in purple. The modified part of the baseline to reach the second KBO is given in green. Maneuvers are illustrated as red stars, KBOs as blue dots. The black dot represents the last planetary flyby.

Figure 4 represents the case where a second KBO encounter is searched for, to be appended to a baseline trajectory that encounters one KBO. First, both the baseline trajectory and the additional KBO trajectory are discretized in time (maneuver date for the baseline trajectory and arrival date for the additional KBO trajectory). Second, the linearized ΔV is calculated for every pair of maneuver and additional KBO arrival epochs. Trajectories with lower ΔV than the chosen threshold are saved,

see Table 1. The time span to seek a new KBO goes from the last KBO encounter to the end of the baseline trajectory.

It is noteworthy that constraining the search to just the end of the baseline does not prematurely prune out KBO sequences as permutations are considered. Regarding time steps, the step size for the KBO orbit is set according to Figure 2. The step size of the baseline trajectory was set to 60 days to reduce computation time at expense of increasing ΔV. As may be seen in Figure 4, the spacecraft only applies one maneuver and never gets back to the baseline.

The TSA can also accommodate for the situation where extra KBOs are sought in the middle of an already established baseline trajectory (rather than purely at the end of a baseline). That is, the case of a trajectory with a fixed flyby sequence but there is some extra propellant to seek bodies in the interim. This TSA variation requires three maneuvers to make the spacecraft return to the baseline trajectory, Figure 5. The third maneuver was set to happen at the next baseline flyby or maneuver epoch to reduce computation time. In Figure 5, the third maneuver occurs at the second flyby epoch.

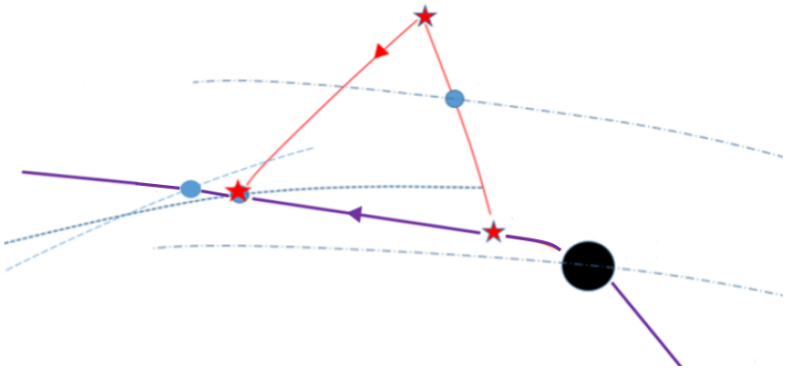

Figure 5. Conceptual image to add an extra (third) KBO out of the baseline trajectory. The baseline trajectory is depicted in purple. The modified part of the baseline to reach the third KBO is given in red. Maneuvers are depicted as red stars, KBOs as blue dots. The black dot represents the last planetary flyby.

This STM-based proximity search may be preceded by a KBO filter to dismiss unreachable KBOs. Such a filter is particularly recommended in problems with large combinatorial spaces and it is applied to every baseline trajectory.

The filter consists of discretizing the baseline trajectory and applies for every resulting grid point a high ΔV^* in different directions using spherical coordinates. Then, for those perturbed trajectories, the maximum and minimum spacecraft position norm and angles are computed from the center of the reference frame. Those six values define the envelope of positions the spacecraft can be in for the set time range, Table 1. Finally, KBOs trajectories are evaluated whether or not they intersect the position envelope. KBOs that do not intersect the envelope in the time range are not considered for the proximity search.

The results provided by the proximity search may be seen in Figures 6 and 7.

[*] A 5-km/s ΔV was applied in this paper.

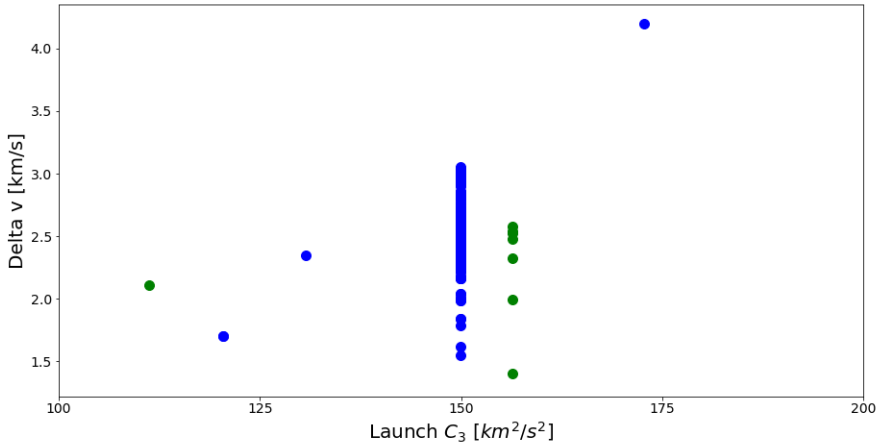

Figure 6. Launch C3 vs total delta-v for all trajectories which encounter three KBOs. Colors refer to the last planet flyby, corresponding green to Uranus and blue to Neptune respectively.

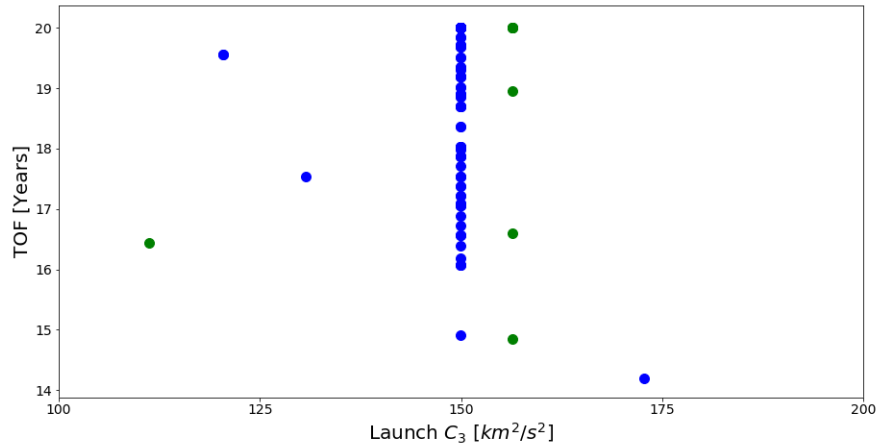

Figure 7. Launch C_3 vs TOF for all trajectories encountering three KBOs. Colors refer to the last planet flyby, corresponding green to Uranus and blue to Neptune respectively.

4. Trajectory optimization of the most promising KBO sequences using EMTG

Trajectories with the lowest ΔV values are used as seeds for pathsolving in EMTG to compute the actual total ΔV value. EMTG performs a stochastic optimization combining Monotonic Basin Hopping and the NLP solver SNOPT[17] .

RESULTS

As a proof of concept, the three-KBO trajectory with the minimum ΔV in Figure 6 was chosen to run on EMTG. The details of this chosen trajectory are given in Tables 6 and 7.

Table 6. Chosen three-KBO trajectory to run in EMTG. Units: JD, km^2/s^2, km/s.

Launch Date	**Launch C3**	**Total ΔV**	**Jupiter Flyby**	**Uranus Flyby**	**1^{st} Maneuver**	**3755735 Flyby**	**2^{nd} Maneuver**	**3^{rd} Maneuver**	**3027724** Flyby	**4^{th} Maneuver**	**2019255 Flyby**
2464156.5	156.36	1.40	2464720.90	2466619.99	2467879.98	2468839.98	2468899.98	2469576.76	2469576.76	2469619.98	2470219.98

Table 7. Maneuver positions of the chosen three-KBO trajectory to run in EMTG. Units: km.

Maneuver number	**X**	**Y**	**Z**
1	-2762720645	2618574361	1424368596
2	-3527389871	3038108348	1901295415
4	-4167919628	3307363487	2058777002

The EMTG results seeded from the chosen three-KBO trajectory are provided in Figure 8. Regarding its baseline two-KBO trajectory, Table 6 removing the last two columns, EMTG outputs Figure 9.

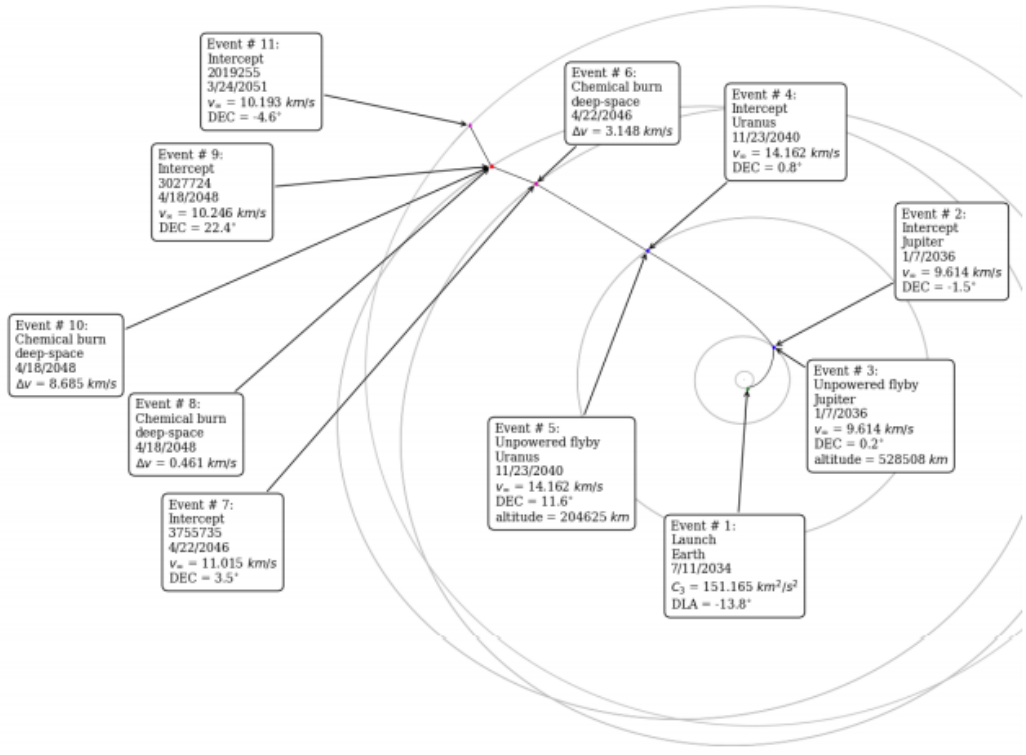

Figure 8. SA output trajectory with three KBOs, total ΔV 12.29 km/s. Seeded from a trajectory with a total ΔV of 1.40 km/s.

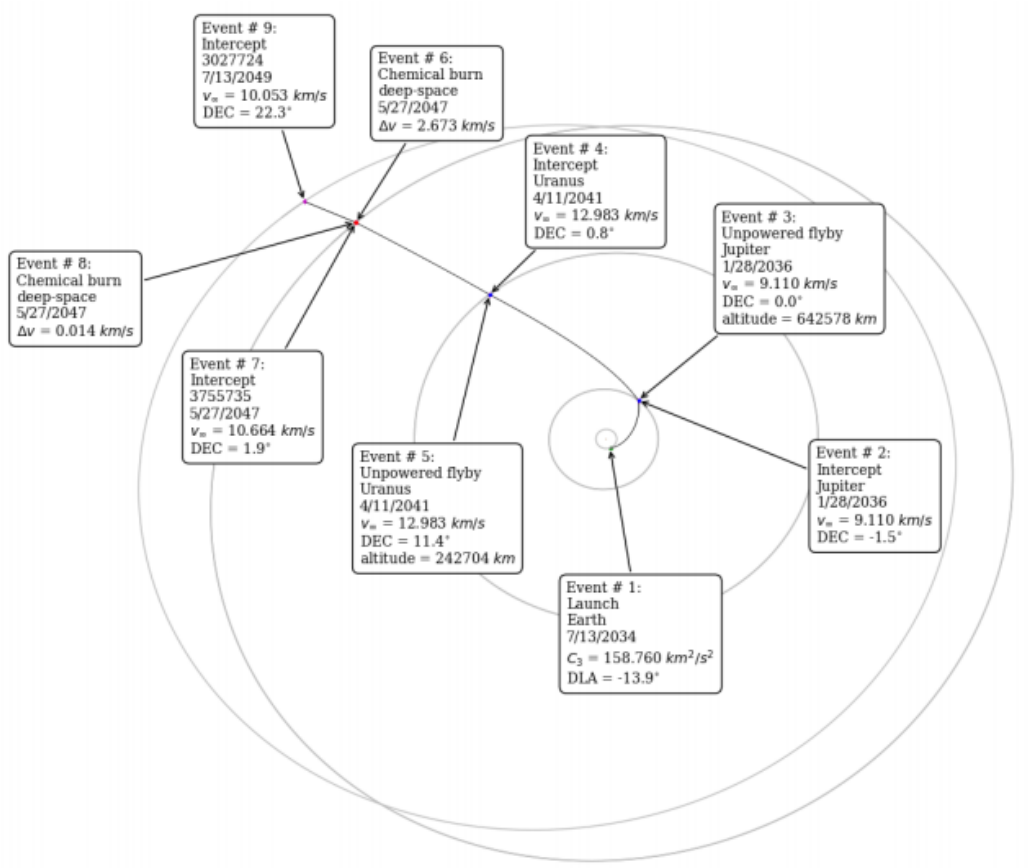

Figure 9. SA output trajectory encountering two KBOs, total ΔV is 2.69 km/s. Seeded from a trajectory with a total ΔV of 1.00 km/s.

As may be seen, the larger the STM-based ΔV results the more misaligned the KBO sequences are. Adding more KBOs tends to increase TSA's ΔV, reducing the chances of getting a feasible trajectory due to a higher misalignment. The two-KBO solution provided by TSA, Figure 9, might be considered for a mission despite the relatively high ΔV of 2.69 km/s.

CONCLUSIONS

The TSA presented in this paper provides a pathfinding workflow for missions to large families of small bodies such as KBOs, NEAs, Jupiter Trojans, or Jovian Moons. An empirical law for the discretization of the target arrival epoch is provided for the outer planets and KBOs. Figures 8 and 9 show the TSA's linearized STM propagation in effect may be interpreted as a reachability metric.

A two-KBO candidate mission is presented using gravity assists at Jupiter and Uranus, which may be flyable with current technology. More KBOs could be encountered if a search is performed in the trajectory vicinities as it was done with New Horizons.

The ΔV values obtained from the proximity search differ from the ones computed with EMTG and have to be interpreted as a reachability metric. Such a difference in ΔV is due to the STM linearization, which may only provide accurate results with very close KBOs. That is why the TSA is expected to find lower ΔVs in regions with a higher density of bodies like missions to NEAs.

FUTURE WORK

Three studies on the TSA are to be conducted and will be included in the journal version of this work. These two studies are:

- Compare the TSA with more traditional distance-based bubble-search heuristic. Likewise the TSA, bubble search is another reachability metric applied to find extra bodies in the vicinity of a baseline trajectory. The bubble search consists of, at every epoch in the baseline trajectory, setting a maximum distance the spacecraft can deviate from the baseline and only focus on the bodies that are within that boundary[5] .
- Run TSA's scenario 2 to find extra targets in the middle of an existing baseline trajectory, such as searching for additional targets along the Lucy trajectory, the first mission to explore the Trojan Asteroids[18] .
- Conduct an in-depth analysis on the ΔV differences between the proximity search and the EMTG results.

REFERENCES

[1] L.-A. McFadden, T. Johnson, and P. Weissman, *Encyclopedia of the solar system*. Elsevier, 2006.

[2] A. E. Petropoulos, J. M. Longuski, and E. P. Bonfiglio, "Trajectories to Jupiter via gravity assists from Venus, Earth, and Mars," *Journal of Spacecraft and Rockets*, Vol. 37, No. 6, 2000, pp. 776–783.

[3] R. P. Russell, "Global search for planar and three-dimensional periodic orbits near Europa," *The Journal of the Astronautical Sciences*, Vol. 54, No. 2, 2006, pp. 199–226.

[4] D. Izzo, V. M. Becerra, D. R. Myatt, S. J. Nasuto, and J. M. Bishop, "Search space pruning and global optimisation of multiple gravity assist spacecraft trajectories," *Journal of Global Optimization*, Vol. 38, No. 2, 2007, pp. 283–296.

[5] B. V. Sarli and Y. Tsuda, "Hayabusa 2 extension plan: Asteroid selection and trajectory design," *Acta Astronautica*, Vol. 138, 2017, pp. 225–232.

[6] B. V. Sarli and Y. Kawakatsu, "Orbit Transfer Optimization for Multiple Asteroid Flybys," *Proceedings of SICE Annual Conference*.

[7] D. H. Ellison, *Robust preliminary design for multiple gravity assist spacecraft trajectories*. PhD thesis, University of Illinois at Urbana-Champaign, 2018.

[8] M. R. Patel, *Automated design of Delta-V gravity-assist trajectories for solar system exploration*. PhD thesis, Purdue University, 1993.

[9] S. W. Napier, J. W. McMahon, and J. A. Englander, "A Multi-Objective, Multi-Agent Transcription for the Global Optimization of Interplanetary Trajectories," *The Journal of the Astronautical Sciences*, Vol. 67, No. 4, 2020, pp. 1271–1299.

[10] T. Crain, R. H. Bishop, W. Fowler, and K. Rock, "Interplanetary flyby mission optimization using a hybrid global-local search method," *Journal of Spacecraft and Rockets*, Vol. 37, No. 4, 2000, pp. 468–474.

[11] M. Vasile and M. Ceriotti, "8 incremental techniques for global space trajectory design," *Spacecraft Trajectory Optimization*, Vol. 29, 2010, p. 202.

[12] M. Vasile and M. Locatelli, "A hybrid multiagent approach for global trajectory optimization," *Journal of Global Optimization*, Vol. 44, No. 4, 2009, pp. 461–479.

[13] J. T. Olympio and D. Izzo, "Designing optimal multi-gravity-assist trajectories with free number of impulses," *International Symposium on Space Flights Dynamics, Toulouse, France. ESA ESTEC*, 2009.

[14] H. S. Coxeter, *Introduction to geometry*. New York, 2nd ed., 1989.

[15] N. J. Strange and J. M. Longuski, "Graphical method for gravity-assist trajectory design," *Journal of Spacecraft and Rockets*, Vol. 39, No. 1, 2002, pp. 9–16.

[16] N. Arora and R. P. Russell, "A fast and robust multiple revolution Lambert algorithm using a cosine transformation," *Paper AAS*, Vol. 13, 2013, p. 728.

[17] R. T. Beeson, J. A. Englander, S. P. Hughes, and M. Schadegg, "An Automatic Medium to High Fidelity Low-Thrust Global Trajectory Toolchain; EMTG-GMAT," 2015.

[18] J. A. Englander, D. H. Ellison, J. A. Englander, D. H. Ellison, K. Williams, J. McAdams, J. M. Knittel, B. Sutter, C. Welch, D. Stanbridge, *et al.*, "Optimization of the Lucy Interplanetary Trajectory via Two-Point Direct Shooting," 2019.